Journal of Materials Chemistry A

COMMUNICATION

View Article Online
View Journal | View Issue

Super-stretchy lithium-ion battery based on carbon nanotube fiber†

Cite this: *J. Mater. Chem. A*, 2014, **2**, 11054

Received 16th April 2014
Accepted 22nd May 2014

DOI: 10.1039/c4ta01878h

www.rsc.org/MaterialsA

Ye Zhang, Wenyu Bai, Jing Ren, Wei Weng, Huijuan Lin, Zhitao Zhang and Huisheng Peng*

Super-stretchy, fiber-shaped lithium-ion batteries with a record strain of 600% are developed by winding two highly aligned carbon nanotube composite fibers. The fiber-shaped battery exhibits high specific capacity, energy density and power density that can be well-maintained under stretching.

Introduction

Stretchable electronic devices, such as circuits,[1] displays,[2] sensors,[3,4] solar cells,[5] are highly required in modern electronics. The lightweight, foldable and wearable format enables several promising applications such as electronic skins to monitor body temperature, blood pressure and other health conditions *in situ* and smart gloves for surgical operations.[6–8] To this end, it is critically important to develop matchable energy storage systems such as lithium-ion batteries. However, conventional lithium-ion batteries have been generally prepared on rigid plates such as copper and aluminum foils that cannot be stretched, which has largely limited their applications.[9–11] On the other hand, to meet the pressing requirement of portable and wearable electronics,[12–14] developing wire-shaped lithium-ion full micro-battery is critical and remains challenging. Compared with the conventional planar structure, the wire-shaped micro-device can be easily woven into flexible textile,[15–18] which had been proposed to represent an effective route to overcome the abovementioned fundamental mismatch in mechanics and form.

Herein, super-stretchy, fiber-shaped lithium-ion batteries with a strain up to 600% have been developed with remarkable electrochemical properties. Two aligned multi-walled carbon nanotube (MWCNT) composite fibers incorporated with active materials were first synthesized with high mechanical strengths, electrical conductivities and electrochemical activities. Then, the stretchable battery was fabricated by winding two composite fibers, which served as positive and negative electrodes on an elastomer substrate, followed by coating with a thin layer of gel electrolyte. No extra metal current collectors and binders were used in these fiber-shaped batteries. The twisted structure of fiber electrodes, elastic substrate and gel electrolyte enabled the super-stretchy property. The specific capacity of 91.3 mA h g^{-1} was achieved and could be maintained up to 88% after stretching by 600%.

State Key Laboratory of Molecular Engineering of Polymers, Department of Macromolecular Science and Laboratory of Advanced Materials, Fudan University, Shanghai 200438, China. E-mail: penghs@fudan.edu.cn

† Electronic supplementary information (ESI) available. See DOI: 10.1039/c4ta01878h

Experimental section

Fabrication of electrodes

$LiMn_2O_4$ particles were synthesized by a hydrothermal method. Lithium hydroxide (0.377 g) was dissolved in deionized water (40 mL), followed by the addition of electrolytic manganese dioxide (1.37 g) to form a black slurry. The slurry was then stirred for 0.5 h at room temperature and then added to glucose (0.20) and deionized water (40 mL) under stirring. The resulting mixture was transferred to a Teflon-lined autoclave (100 mL) for hydrothermal treatment at 200 °C for 24 h. The product was filtered and washed with deionized water, followed by drying at 120 °C for 24 h. $Li_4Ti_5O_{12}$ particles were synthesized by a solid-state method. TiO_2 and Li_2CO_3 with a molar ratio of 2.5 was mixed and heated at 800 °C for 24 h in a N_2 atmosphere, followed by a ball-milling treatment for 20 h to form $Li_4Ti_5O_{12}$ nanoparticles. Aligned MWCNT arrays were synthesized by chemical vapor deposition in a quartz tube furnace with a diameter of 2 inches. Fe (1.5 nm)/Al_2O_3 (5 nm) deposited on silica wafer by electron-beam evaporation was used as the catalyst, and ethylene with a flowing rate of 90 sccm was used as the carbon precursor that was mixed with H_2 (30 sccm) and Ar (400 sccm) as the carrier gas. Growth occurred at 740 °C for 10 min. MWCNT sheets were then pulled out of the array with a width of ~2 cm. Two MWCNT sheets could be further stacked along the MWCNT length. To prepare a $LiMn_2O_4$/MWCNT composite fiber, $LiMn_2O_4$ (0.075 g) and MWCNT powder (0.075 g) were added to *N*,*N*-dimethylformamide (15 mL) to produce a

solution with a concentration of ~0.5%. The resulting solution was then coated onto the stacked MWCNT sheets, followed by scrolling into a fiber. The $Li_4Ti_5O_{12}$/MWCNT composite fiber could be prepared by a similar procedure by coating a $Li_4Ti_5O_{12}$ (0.075 g)/*N*,*N*-dimethylformamide (15 mL) solution, though no MWCNT powder was mixed in the solution. In addition to MWCNT/$LiMn_2O_4$ and $Li_4Ti_5O_{12}$/MWCNT composite fibers, this strategy can be extended to synthesize other composite fibers with a variety of nanoparticles.

Gel electrolyte

Methylene chloride and acetone were mixed first (40/1, w/w), followed by the addition of poly (ethylene oxide) ($M_w \sim 600\,000$, 0.35 g), succinonitrile (0.35 g) and lithium bis(trifluoromethane)sulfonimide (0.30 g). The gel electrolyte was produced after stirring for 5 h. All procedures were performed in a glove box filled with dry argon gas.

Fabrication of lithium-ion batteries

Two ends of a polydimethylsiloxane (PDMS) fiber were first fixed onto the motors (Fig. 1). A MWCNT/$LiMn_2O_4$ composite fiber and a MWCNT/$Li_4Ti_5O_{12}$ composite fiber were then fixed together in parallel with a distance of ~1 mm to prevent short circuit, and further adhered to the PDMS fiber with an angle of θ (θ is determined by the radius of the substrate which will be discussed below). The motors were steadily rotated such that the two fiber electrodes were wound onto the PDMS fiber. During the winding process, the helical angle of θ was maintained as the same. The resulting electrode assembly was coated with a layer of gel electrolyte and PDMS membrane to seal the battery.

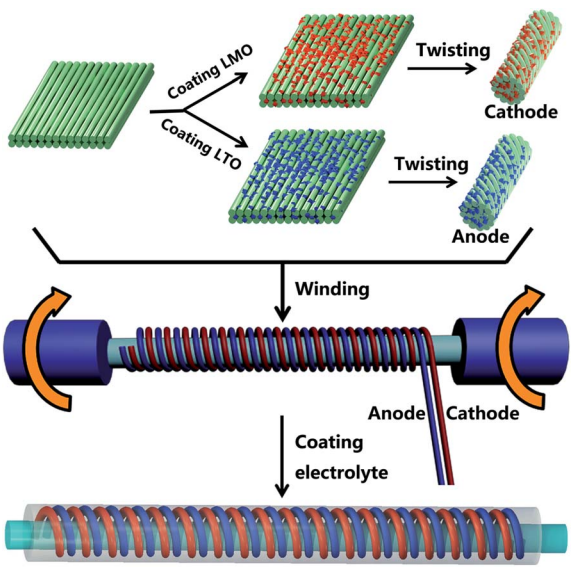

Fig. 1 Schematic illustration of the fabrication of the super-stretchy lithium-ion battery based on the MWCNT/$LiMn_2O_4$ composite fiber as a positive electrode and MWCNT/$Li_4Ti_5O_{12}$ composite fiber as a negative electrode.

Characterization

The structures were characterized by scanning electron microscopy (SEM, Hitachi FE-SEM S-4800 operated at 1 kV) and X-ray diffraction (XRD, Bruker AXS D8). Galvanostatic charge–discharge measurements were made at current densities of 0.05 and 0.1 mA cm^{-1} and a voltage range of 1.5 to 3.2 V. The cyclic performance was recorded at a current density of 0.1 mA cm^{-1}. The mass and length specific capacities (C_m and C_l) were calculated according to the equations of $C_m = (I \times \Delta t)/L$ and $C_l = (I \times \Delta t)/m$, respectively, where I, Δt, L and m represent the applied current, discharge time, effective length of the fiber battery and mass of negative electrode. The abovementioned measurements were made at an ARBIN electrochemical workstation (MSTAT-5V/10 mA/16Ch). The mechanical measurements were performed at HY-0350, Shanghai Hengyi Testing Instruments Co. LTD.

Results and discussion

Spinnable MWCNT arrays with a height of ~240 μm were synthesized by chemical vapor deposition.[19] The diameter of MWCNTs was appropriately 10 nm. Then, aligned MWCNT sheets with a thickness of ~18 nm were drawn out of the array with a width of ~2 cm. Two stacked MWCNT sheets along the drawing direction were first coated with $LiMn_2O_4$ or $Li_4Ti_5O_{12}$ and then twisted to form aligned MWCNT/$LiMn_2O_4$ or MWCNT/$Li_4Ti_5O_{12}$ composite fibers, respectively. The MWCNT/$LiMn_2O_4$ and MWCNT/$Li_4Ti_5O_{12}$ composite fibers were further wound onto an elastic fiber to serve as positive and negative electrodes, respectively. A thin layer of gel electrolyte was finally coated on and between the two electrodes to produce the fiber-shaped battery (Fig. 1). The gel electrolyte was composed of poly(ethylene oxide), lithium bis(trifluoromethane)sulfonimide and plasticizer succinonitrile.[20] Succinonitrile was used to suppress the crystallinity of poly(ethylene oxide) and promote the dissociation of lithium bis(trifluoromethane)sulfonimide, thus achieving higher carrier mobility. As expected, this electrolyte exhibited electrical conductivities of the level of 10^{-3} S cm^{-1},[20] which enabled its use as both electrolyte and separator.

Fig. 2a and b show scanning electron microscopy (SEM) images of the MWCNT/$LiMn_2O_4$ (weight percentage of 83.6% for the $LiMn_2O_4$) and MWCNT/$Li_4Ti_5O_{12}$ (weight percentage of 57.7% for the $Li_4Ti_5O_{12}$) composite fibers, respectively. The abovementioned weight percentages were used in the following discussion if not specified. The fiber diameters were appropriately 160 and 130 μm, respectively (Fig. S1†). For both the composite fibers, MWCNTs were highly aligned with the metal oxide nanoparticles well dispersed among them, which can also be verified by cross-sectional SEM images (Fig. S2 and S3†). The $LiMn_2O_4$ and $Li_4Ti_5O_{12}$ nanoparticles were analyzed by X-ray diffraction (Fig. S4†). The characteristic peaks indicated a spinel phase for both of them. Both $LiMn_2O_4$ and $Li_4Ti_5O_{12}$ were physically attached on the surfaces of aligned MWCNTs. Here, no obvious shifts were found in Raman and FTIR spectra for both MWCNT/$LiMn_2O_4$ and MWCNT/$Li_4Ti_5O_{12}$ composite fibers (Fig. S6 and S7†). The MWCNT/$LiMn_2O_4$ and MWCNT/

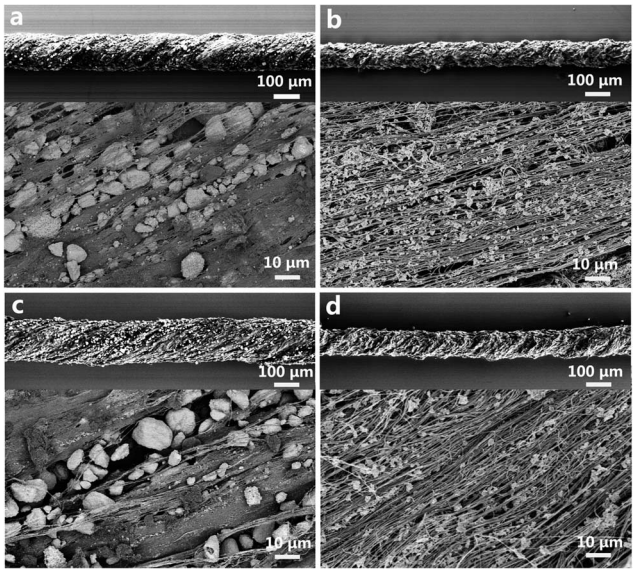

Fig. 2 (a and b) Scanning electron microscopy (SEM) images of MWCNT/$LiMn_2O_4$ and MWCNT/$Li_4Ti_5O_{12}$ composite fibers at different magnifications, respectively. (c and d) SEM images of MWCNT/$LiMn_2O_4$ and MWCNT/$Li_4Ti_5O_{12}$ composite fibers at different magnifications after stretching by 200%, respectively.

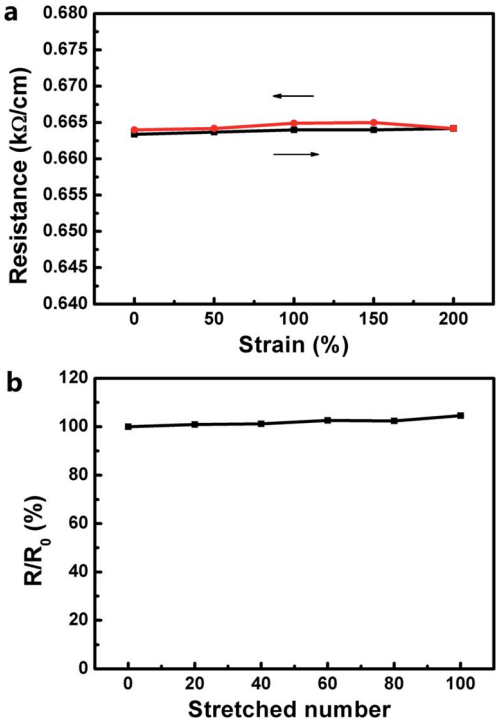

Fig. 3 (a) Changes in resistances of the negative electrode during a stretching and releasing process with a strain of 200%. (b) Dependence of resistances on stretched number at the strain of 200%. R_0 and R correspond to electrical resistances before and after stretching, respectively.

$Li_4Ti_5O_{12}$ composite fibers were further wound onto an elastic polydimethylsiloxane fiber to serve as positive and negative electrodes, respectively. No obvious destruction in the structure was observed for the two composite fiber electrodes after stretching by 200% (Fig. 2c and d). The electrical resistances were further traced during the stretching process to verify the structural integrity of the fiber electrodes (Fig. 3 and S8†). It was revealed that the resistances varied less than 1% at the strain of 200% and less than 5% for both the composite fibers after stretching for 100 cycles.

The electrochemical performance of the composite fiber electrode was examined in a half-cell with a lithium wire as the counter electrode. Fig. S9† showed the first three cycles of the charge and discharge curves of MWCNT/$LiMn_2O_4$ and MWCNT/$Li_4Ti_5O_{12}$ composite fibers at a current density of 0.1 mA cm^{-1}. The average discharge voltages were 3.7 and 1.3 V, respectively; the reversible discharge capacities were found to be 0.42 and 0.21 mA h m^{-1}, respectively. For conventional lithium-ion battery with carbon as the negative electrode, negative capacity is in excess to prevent the deposition of Li on the surface of the negative electrode. Promisingly, it is not necessary for the negative capacity to be excessive here because lithium deposition will be intrinsically inhibited due to high voltage plateau of $Li_4Ti_5O_{12}$. In addition, the stable structure of $Li_4Ti_5O_{12}$ during the charging and discharging process also enables a good capacity retention in the negative electrode, which further provides the full battery with a high cyclic performance.[21,22] To determine the maximal load of electrode materials, the weight percentage of $LiMn_2O_4$ nanoparticles in the composite fibers was increased to 87%. Numerous nanoparticles were found on the surface of the composite fiber, and the alignment of MWCNTs was also largely decreased (Fig. S10†). During the charging and discharging process, the particles on the surface peeled off from the fibers, which led to a larger capacity decay compared with a weight percentage of 83.6% (Fig. S11†). Similarly, the maximal load of $Li_4Ti_5O_{12}$ nanoparticles was determined to be 57.7% to achieve a matchable capacity between the two electrodes. The abovementioned results show that the two composite fiber electrodes can be well-matched in both capacity and voltage, and may be assembled into an efficient full battery.

The full fiber-shaped battery was charged and discharged between 1.5 and 3.2 V for one cycle at a current density of 0.02 mA cm^{-1} prior to the cyclic measurement. Typical voltage profiles with increasing cycle numbers at a current density of 0.1 mA cm^{-1} are shown in Fig. 4a. The average discharge voltage was 2.2 V, and the initial discharge capacity reached 91.3 mA h g^{-1} based on the entire negative electrode (*i.e.*, the total weight of MWCNT and $Li_4Ti_5O_{12}$), which was consistent with those of the planar batteries reported previously.[21–25] Planar electrodes based on carbon nanocomposites were previously explored in transparent[25] and foldable[26] batteries. A transparent lithium ion battery with $LiMn_2O_4$ and $Li_4Ti_5O_{12}$ nanoparticles in the two electrodes demonstrated a specific capacity of 100 mA h g^{-1}. Note that foldable lithium ion paper batteries[26] exhibited specific capacities ranging from 103 to 113 mA h g^{-1}, while a stretchable polymer/CNT composite electrode[27] produced specific capacity of 75 mA h g^{-1}. Therefore, the stretchable fiber-shaped lithium ion batteries share the same level of specific capacities as their flexible planar counterparts, including both

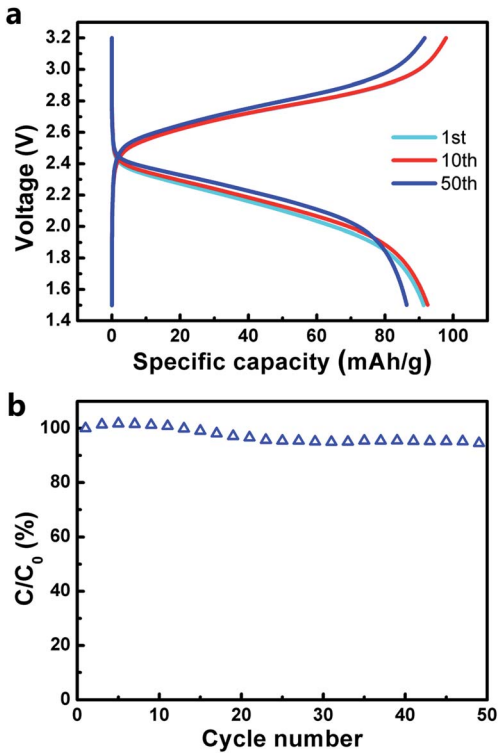

Fig. 4 (a) Charge and discharge profiles of a fiber-shaped battery with increasing cycle numbers at a current density of 0.1 mA cm^{-1}. (b) Dependence of specific capacity on cycle number. C_0 and C correspond to the specific capacity at the first and following cycle, respectively.

non-stretchable and stretchable batteries. This high capacity was derived from the composite fiber electrode where MWCNTs served as both skeletons and current collectors for charge transports without non-electrochemically active metal current collectors and binders. The initial discharge capacity could be also transformed to 0.36 mA h m^{-1} on the basis of battery length.

The two composite fibers were wound onto an elastic fiber (radius ~1 mm) with an angle of θ to form a periodically-arranged double thread (Fig. 1 and S16†). The pitch distance (d) was maintained at 1 mm. The length of the full battery (L_2) may be calculated from the length of the fiber electrodes (L_1) by equation of $L_2 = L_1 \times \cos\theta$. Therefore, the length specific capacity was increased by $(1/\cos\theta - 1)$ compared with the straight fiber electrode. The Coulomb efficiency of the first cycle was 92.1%. The capacity was maintained by 95% after 50 cycles (Fig. 4b) and 78% after 100 cycles (Fig. S12†), verifying the abovementioned explanation that the excessive positive capacity ensured a high cyclic performance. The fiber-shaped battery can be well reproduced with stable electrochemical performances (Fig. S13†). The energy density and power density of this fiber-shaped battery achieved 10.6 mW h cm^{-3} and 0.294 W cm^{-3} based on the volume of the two electrodes and 30 W h kg^{-1} and 830 W kg^{-1} based on the weight of the two electrodes.

The fiber-shaped lithium-ion battery was highly flexible and stretchable. It can be wound onto a glass rod (Fig. S14†) and bent into various angles without the obvious decrease in electrochemical performance. As shown in Fig. 5a, the specific capacity can be maintained by 92% even at a bending angle of 180°, and there were no obvious changes in the charge and discharge profiles before and after bending for 100 and 200 cycles at the angle of 90° (Fig. 5b). Furthermore, this fiber-shaped battery can be stretched by over 200% (Fig. S15†). The fiber electrode was coated with a layer of gel electrolyte, which also served as a separator, to avoid a direct contact between the anode and cathode during the stretching process. The electrochemical properties of the fiber-shaped lithium ion battery were further studied with increasing strains up to 200%. The shapes of charge–discharge curves were well-maintained (Fig. 5c), and no obvious decrease in capacity was observed, *e.g.*, the specific capacity was maintained at over 93% at the strain of 200% (Fig. 5d). In addition, the specific capacity was maintained at above 90% after stretching for 100 cycles (Fig. 5e). The stretched fiber-shaped battery with a strain of 100% was also investigated for cyclic stability, and the capacities were maintained to be above 90% after 50 charge–discharge cycles (Fig. 5f). These results demonstrate that the fiber-shaped lithium ion battery

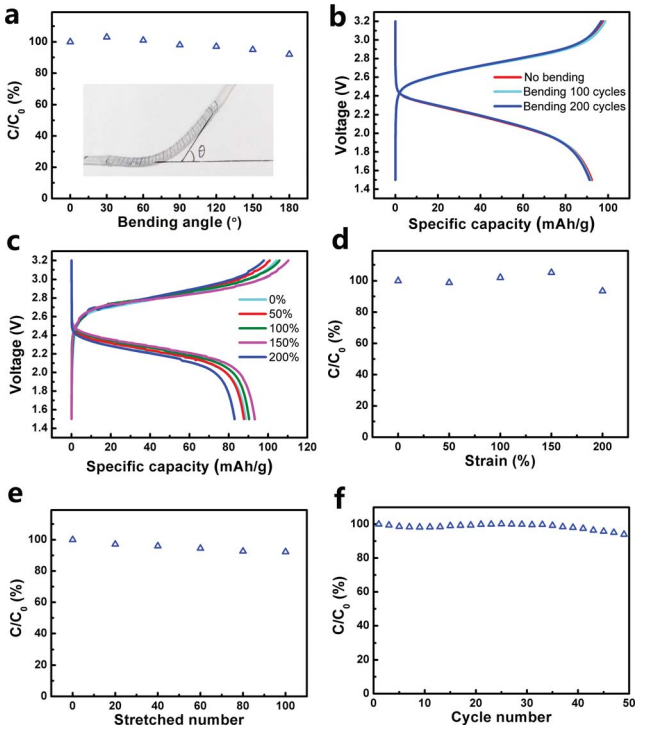

Fig. 5 (a) Dependence of specific capacity on bent angle. C_0 and C correspond to specific capacities before and after bending, respectively. (b) Charge and discharge profiles before and after bending for 100 and 200 cycles at a current density of 0.1 mA cm^{-1}. (c) Charge and discharge profiles with strains increasing from 0%, 50%, 100% and 150% to 200% at a current density of 0.1 mA cm^{-1}. (d and e) Dependence of the ratio of specific capacity on strain and stretched number (at a strain of 100%), respectively. C_0 and C correspond to specific capacity before and after stretching, respectively. (f) Dependence of the ratio of specific capacity on cycle number at a strain of 100%. C_0 and C correspond to the specific capacity at the first and following cycle, respectively.

exhibits a stable electrochemical performance under stretching, which may be attributed to the twisted structure of fiber electrodes and the stretchability of the substrate and gel electrolyte. The electrodes were wound onto an elastic substrate to form a spring-like structure, and this structure was further anchored by the coated gel electrolyte. When the battery was stretched, the spring-like structure of the two electrodes was maintained with increasing pitch distances. The structure of the nanocomposite electrode remained unchanged during stretching under SEM (Fig. 2).

To further verify the highly stretchable property (Fig. 6a and b), the fiber-shaped battery was used to power a red light-emitting diode (LED) under stretching (Fig. 6c). No obvious change in brightness was observed for the LED when the battery was continuously stretched to a high strain of 200%. In addition, compared with stretchable planar structure batteries,[27,28] these fiber-shaped batteries can be easily scaled up with an applicable length and woven into textiles with different shapes such as a bracelet (Fig. 6d) and knitted sweater (Fig. 6e and f) to achieve better adaptability to the movement of the body. The obtained battery textile can be well-accommodated with the folding and stretching of the sweater (Fig. 6g and h), which shows its promising applications in wearable devices.

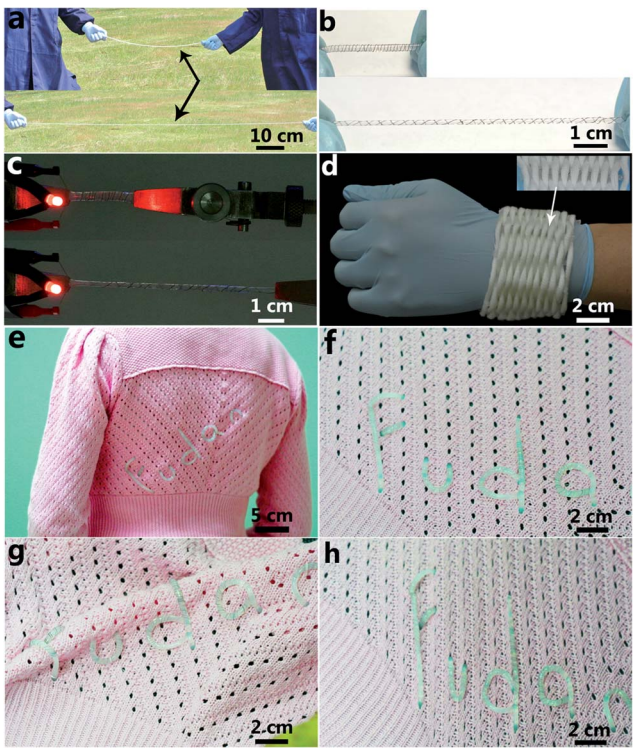

Fig. 6 (a and b) Photographs of stretchable fiber-shaped batteries with lengths of 40 and 3 cm before and after stretching by 200%, respectively. (c) Photograph of a stretchable fiber-shaped battery being used to power a LED before and after stretching by 200%. (d) Photograph of stretchable fiber-shaped batteries being woven into a bracelet textile. (e–h) Photographs of stretchable fiber-shaped batteries being woven into a knitted sweater (e and f) and under folding (g) and stretching (h).

The maximal strain of the twisted fiber-shaped battery during stretching is further investigated in Fig. S16.† The helical angle between the wound fiber electrode and fiber substrate, radius of the fiber substrate, pitch distance between two fiber electrodes, length of the fiber electrode, length of the battery are defined as θ, r, d, L_1 and L_2, respectively. Two equations are thus obtained, *i.e.*, $\tan\theta = 2\pi r/2d$ and $\cos\theta = L_2/L_1$. Obviously, the strain of the battery (ε) is increased with decreasing θ. In an ideal case, the fiber-shaped battery is stretched to produce a length of L_1, and the maximum strain (ε_{max}) may be expressed by $\varepsilon_{max} = (L_1 - L_2)/L_2$. After integration of the abovementioned three equations, the maximal strain can be finally calculated by:

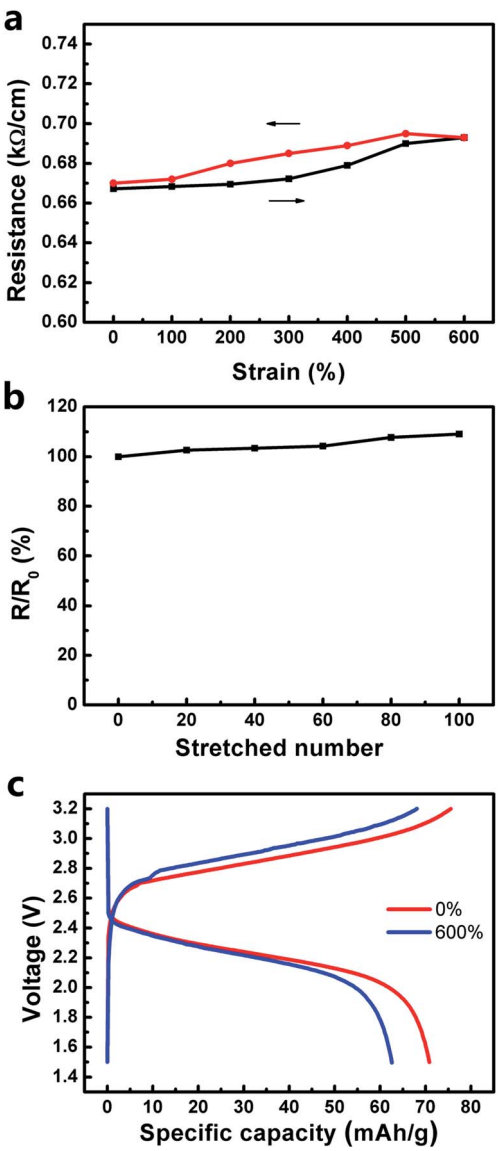

Fig. 7 (a) Changes in resistances for the negative electrode during a stretching and releasing process at a strain of 600%. (b) Dependence of resistances on stretched number at the strain of 600%. R_0 and R correspond to resistances before and after stretching, respectively. (c) Charge and discharge profiles before and after stretching to 600% at a current density of 0.1 mA cm^{-1}.

$$\varepsilon_{max} = \sqrt{\frac{\pi^2 r^2}{d^2} + 1} - 1$$

For a given pitch distance, ε_{max} increases with the increasing radius of the fiber substrate. This simplified model provides a general and effective strategy to further enhance the stretchability of the twisted fiber-shaped battery. For instance, when the radius of the fiber substrate was increased from 1 to 2.5 mm, the maximal strain was considerably improved to 600% (Fig. S17†). The electrical resistance of the MWCNT/$Li_4Ti_5O_{12}$ composite fiber was slightly increased by 3.86% at a strain of 600% and by 6.30% after stretching for 100 cycles (Fig. 7a and b); the resistance of the MWCNT/$LiMn_2O_4$ composite fiber was increased by 5.80% at the strain of 600% and by 15% after stretching for 100 cycles (Fig. S18†). As expected, the shapes of the charge–discharge curves remained almost unchanged (Fig. 7c), and the specific capacity was maintained at over 88% at a strain of 600%.

Conclusion

In summary, we developed a super-stretchy fiber-shaped lithium-ion battery that can be stretched up to 600% by exploring novel composite fiber materials and designing a new twisted structure. The fiber-shaped battery exhibits high specific capacity, energy density and power density, which can be well-maintained under stretching. These super-stretchy fiber-shaped batteries have been further woven into elastic energy storage textiles, which are particularly promising to power various wearable and portable electronic devices.

Acknowledgements

This work was supported by MOST (2011CB932503), NSFC (21225417), STCSM (12nm0503200), the Fok Ying Tong Education Foundation, the Program for Special Appointments of Professors at Shanghai Institutions of Higher Learning, and the Program for Outstanding Young Scholars from the Organization Department of the CPC Central Committee.

References

1 D. H. Kim, J. H. Ahn, W. M. Choi, H. S. Kim, T. H. Kim, J. Z. Song, Y. G. Y. Huang, Z. J. Liu, C. Lu and J. A. Rogers, *Science*, 2008, **320**, 507.
2 T. Sekitani, H. Nakajima, H. Maeda, T. Fukushima, T. Aida, K. Hata and T. Someya, *Nat. Mater.*, 2009, **8**, 494.
3 T. Yamada, Y. Hayamizu, Y. Yamamoto, Y. Yomogida, A. Izadi-Najafabadi, D. N. Futaba and K. Hata, *Nat. Nanotechnol.*, 2011, **6**, 296.
4 D. J. Lipomi, M. Vosgueritchian, B. C. K. Tee, S. L. Hellstrom, J. A. Lee, C. H. Fox and Z. N. Bao, *Nat. Nanotechnol.*, 2011, **6**, 788.
5 D. J. Lipomi, B. C. K. Tee, M. Vosgueritchian and Z. N. Bao, *Adv. Mater.*, 2011, **23**, 1771.
6 M. Kaltenbrunner, T. Sekitani, J. Reeder, T. Yokota, K. Kuribara, T. Tokuhara, M. Drack, R. Schwodiauer, I. Graz, S. Bauer-Gogonea, S. Bauer and T. Someya, *Nature*, 2013, **499**, 458.
7 L. Cai, L. Song, P. S. Luan, Q. Zhang, N. Zhang, Q. Q. Gao, D. Zhao, X. Zhang, M. Tu, F. Yang, W. B. Zhou, Q. X. Fan, J. Luo, W. Y. Zhou, P. M. Ajayan and S. S. Xie, *Sci. Rep.*, 2013, **3**, 3402.
8 T. Someya, T. Sekitani, S. Iba, Y. Kato, H. Kawaguchi and T. Sakurai, *Proc. Natl. Acad. Sci. U. S. A.*, 2004, **101**, 9966.
9 H.-G. Jung, M. W. Jang, J. Hassoun, Y.-K. Sun and B. Scrosati, *Nat. Commun.*, 2011, **2**, 516.
10 W. Weng, H. Lin, X. Chen, J. Ren, Z. Zhang, L. Qiu, G. Guan and H. Peng, *J. Mater. Chem. A*, 2014, **2**, 9306.
11 W. Wei, S. Yang, H. Zhou, I. Lieberwirth, X. Feng and K. Müllen, *Adv. Mater.*, 2013, **25**, 2909.
12 J. Ren, L. Li, C. Chen, X. L. Chen, Z. B. Cai, L. B. Qiu, Y. G. Wang, X. R. Zhu and H. S. Peng, *Adv. Mater.*, 2013, **25**, 1155.
13 H. Lin, W. Weng, J. Ren, L. Qiu, Z. Zhang, P. Chen, X. Chen, J. Deng, Y. Wang and H. Peng, *Adv. Mater.*, 2014, **26**, 1217.
14 Y. Kwon, S. Woo, H. Jung, H. K. Yu, K. Kim, B. H. Oh, S. Ahn, S. Lee, S. Song, J. Cho, H. Shin and J. Y. Kim, *Adv. Mater.*, 2012, **24**, 5192.
15 J. Ren, W. Y. Bai, G. Z. Guan, Y. Zhang and H. S. Peng, *Adv. Mater.*, 2013, **25**, 5965.
16 M. D. Lima, S. Fang, X. Lepró, C. Lewis, R. O. Robles, J. C. González, E. C. Martínez, M. E. Kozlov, J. Oh, N. Rawat, C. S. Haines, M. H. Haque, V. Aare, S. Stoughton, A. A. Zakhidov and R. H. Baughman, *Science*, 2011, **331**, 51.
17 Y. H. Lee, J. S. Kim, J. Noh, I. Lee, H. J. Kim, S. Choi, J. Seo, S. Jeon, T. S. Kim, J. Y. Lee and J. W. Choi, *Nano Lett.*, 2013, **13**, 5753.
18 J. Ren, Y. Zhang, W. Bai, X. Chen, Z. Zhang, X. Fang, W. Weng, Y. Wang and H. Peng, *Angew. Chem. Int. Ed.*, 2014, **53**, DOI: 10.1002/anie.201402388.
19 T. Chen, Z. Cai, L. Qiu, H. Li, J. Ren, H. Lin, Z. Yang, X. Sun and H. Peng, *J. Mater. Chem. A*, 2013, **1**, 2211.
20 M. Echeverri, N. Kim and T. Kyu, *Macromolecules*, 2012, **45**, 6068.
21 X. K. Huang, M. Lin, Q. S. Tong, X. H. Li, Y. Ruan and Y. Yang, *J. Power Sources*, 2012, **202**, 352.
22 H. F. Xiang, X. Zhang, Q. Y. Jin, C. P. Zhang, C. H. Chen and X. W. Ge, *J. Power Sources*, 2008, **183**, 355.
23 S. Brutti, V. Gentili, P. Reale, L. Carbone and S. Panero, *J. Power Sources*, 2011, **196**, 9792.
24 H. G. Jung, M. W. Jang, J. Hassoun, Y. K. Sun and B. Scrosati, *Nat. Commun.*, 2011, **2**, 516.
25 Y. Yang, S. Jeong, L. B. Hu, H. Wu, S. W. Lee and Y. Cui, *Proc. Natl. Acad. Sci. U. S. A.*, 2011, **108**, 13013.
26 Q. Cheng, Z. Song, T. Ma, B. B. Smith, R. Tang, H. Yu, H. Jiang and C. K. Chan, *Nano Lett.*, 2013, **10**, 4969.
27 H. Lee, J. K. Yoo, J. H. Park, J. H. Kim and K. Kang, *Adv. Energy Mater.*, 2012, **2**, 976.
28 S. Xu, Y. Zhang, J. Cho, J. Lee, X. Huang, L. Jia, J. A. Fan, Y. Su, J. Su, H. Zhang, H. Cheng, B. Lu, C. Yu, C. Chuang, T. Kim, T. Song, K. Shigeta, S. Kang, C. Dagdeviren, I. Petrov, P. V. Braun, Y. Huang, U. Paik and J. A. Rogers, *Nat. Commun.*, 2013, **4**, 1543.